

Effect of positron space charge on operation of an antihydrogen trap

C. A. Ordonez

Department of Physics, University of North Texas, Denton, Texas 76203, USA

(Received 3 April 2007; published 16 July 2007)

Experimental conditions have recently been reported [G. Andresen *et al.*, Phys. Rev. Lett. **98**, 023402 (2007)] that are relevant to the prospect of trapping antihydrogen atoms. An analysis of the experimental conditions indicates that positron space charge can have an important effect. The fraction of antiprotons that have an energy suitable for antihydrogen trapping can be reduced by drifts caused by the presence of positron space charge.

DOI: 10.1103/PhysRevE.76.017402

PACS number(s): 52.27.Jt, 52.25.Xz, 52.20.Dq

During the past few years, two international collaborations ATHENA and ATRAP reported using nested Penning traps to produce neutral antimatter in the form of antihydrogen [1–4]. More recently, the ALPHA Collaboration reported operation of a Penning trap under conditions that “should simulate the situation immediately before particle mixing in an antihydrogen synthesis or trapping cycle” [5]. A theoretical analysis of the conditions reported by the ALPHA Collaboration is presented here regarding the effect of positron space charge on the prospect of trapping antihydrogen atoms that are produced under such conditions.

Figure 1 illustrates the trap configuration and the applied electric potential profiles considered here. Eight cylindrical electrodes are aligned end-to-end along a common axis of symmetry. A cylindrical coordinate system with coordinates (r, θ, z) is defined such that the z axis coincides with the axis of symmetry. Each electrode has a length L and an inner wall radius r_w . The distance between adjacent electrodes is considered to be negligible compared to the length of each electrode. Eight voltages, $V_4, V_t, V_g, V_2, V_0, V_0, V_2,$ and V_4 , are applied to the eight electrodes. The antiprotons and positrons are shown confined within separate volumes in Fig. 1(a), and each species is assumed to have a confinement radius r_p . The voltage V_g is then changed such that the axial confinement volume of the antiprotons will overlap the positron confinement volume, as illustrated in Fig. 1(b). The parameters before V_g is changed are taken to be those reported by the ALPHA Collaboration regarding positron and antiproton confinement in a Penning trap in the presence of a minimum- B magnetic field [5]. Unless noted otherwise, the following parameters are used: electrode dimensions $L=20$ mm and $r_w=22.3$ mm, a temperature of the trap electrodes in the mixing region of 4 K, $N_+ \lesssim 3 \times 10^7$ positrons, several thousand antiprotons, a solenoidal magnetic field of strength $B=1$ T that defines the bottom of the magnetic well, and a maximum energy $E_{\max}=0.4k$ for an antihydrogen atom in a weak-magnetic-field-seeking ground state to remain trapped within the magnetic well, where k is Boltzmann’s constant in SI units. E_{\max} is considered hereafter to be the maximum desirable antiproton kinetic energy for forming antihydrogen that may remain trapped within the magnetic well. A positron temperature equal to the electrode temperature $T_+=4$ K is used, with the assumption that cyclotron radiation effectively reduces the positron temperature to that of the trap electrodes. It is not clear how cold the antiproton temperature

may be. The importance of accurately determining (either experimentally or theoretically) the antiproton temperature becomes apparent by calculating the fraction of antiprotons with kinetic energies less than E_{\max} . For antiprotons having a nondrifting Maxwellian velocity distribution associated with a temperature T_- , the fraction is given by

$$f_t = \operatorname{erf}\left(\sqrt{\frac{E_{\max}}{kT_-}}\right) - 2\sqrt{\frac{E_{\max}}{\pi kT_-}} \exp\left(-\frac{E_{\max}}{kT_-}\right), \quad (1)$$

where erf is the error function. Equation (1) gives $f_t=0.022$ for $T_-=4$ K, and $f_t=0.0059$ for $T_-=10$ K. An antiproton temperature equal to the electrode temperature $T_-=4$ K is optimistically assumed hereafter.

In Fig. 1(a), the antiprotons are illustrated as initially confined within a temporary well located under the electrode with applied voltage V_t . To achieve positron and antiproton

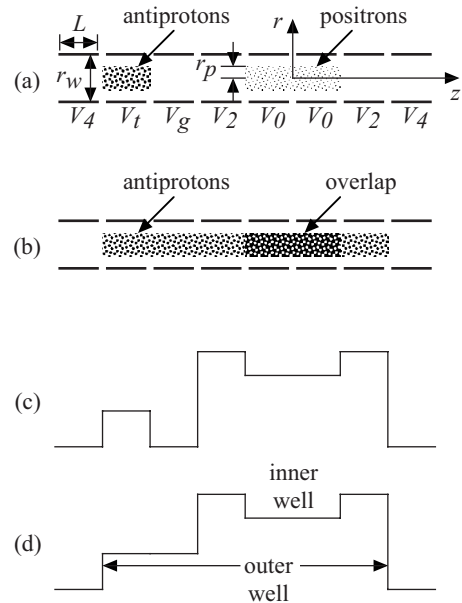


FIG. 1. The trap configuration (a), (b) and electric potential profiles that could be produced axially along the electrode wall (c), (d). The confinement volumes for the positrons and antiprotons do not overlap (a) during the time an initial electric potential profile is applied (c). The two confinement volumes overlap (b) after the electric potential profile is changed (d). A magnetic field provides radial confinement of each species.

mixing, the voltage V_g , which serves as an electric gate, is changed so as to change the electric potential profile along the wall from that shown in Fig. 1(c) to that shown in Fig. 1(d). Figure 1(d) illustrates an electric potential along the wall that produces a nested well configuration consisting of an “inner well” and an inverted “outer well.” If the conditions are right, the antiproton confinement volume overlaps the positron confinement volume at all radial positions $r < r_p$, after V_g is changed. The effect of both the radial electric field produced by the positron plasma and the radial dependence of the inner well depth are now considered.

Antiprotons that enter the positron plasma will be subjected to the radial electric field produced by the positron plasma, and the antiprotons will experience an azimuthal $\mathbf{E} \times \mathbf{B}$ drift. An antiproton’s azimuthal drift velocity in the infinite cylindrical column approximation is given by

$$v_\theta = \frac{eBr}{2m_-} \left(\sqrt{1 + \frac{2m_- \Delta n}{\epsilon_0 B^2}} - 1 \right). \quad (2)$$

Here, $\Delta n = n_+ - n_-$, n_+ and n_- are the positron and antiproton densities, which are approximated as being radially uniform, m_- is the antiproton mass, e is the positron charge, and ϵ_0 is the permittivity of free space. For simplicity, the magnetic field strength throughout the positron plasma is approximated as being uniform and equal to the solenoidal magnetic field strength B . Two additional approximations are useful. They are that the positron density is given by $n_+ = N_+ / (2\pi r_p^2 L)$, and that $\Delta n = n_+$, with the assumption that the antiproton density within the positron plasma is negligible compared to the positron density. Let $K_\theta = \frac{1}{2} m_- v_\theta^2$ denote the antiproton kinetic energy associated with an antiproton’s azimuthal drift motion, where v_θ is given by Eq. (2). The fraction of antiprotons (within the positron plasma) for which K_θ is less than E_{\max} is given by

$$f_\theta = 8m_- E_{\max} \left[eBr_p \left(\sqrt{1 + \frac{2m_- \Delta n}{\epsilon_0 B^2}} - 1 \right) \right]^{-2}. \quad (3)$$

The space charge of the positron plasma causes there to be a difference in the electric potential between the radial center of the positron plasma and any other radial position within the positron plasma. In the infinite cylindrical column approximation, the difference in potential between $r=0$ and r is given by $e\Delta n r^2 / (4\epsilon_0)$ for $r \leq r_p$. The difference in potential causes the inner well to be 1.1 V deeper at $r=r_p$ than at $r=0$ for $N_+ = 3 \times 10^7$ [with $\Delta n = n_+ = N_+ / (2\pi r_p^2 L)$]. The radial dependence of the inner well depth can affect the antiproton kinetic energy. It is convenient to define an axial drift velocity, hereafter denoted v_z , as the local average of the magnitude of the z component of the antiproton velocity, excluding any contribution associated with thermal motion. It is also convenient to make two assumptions. First, assume that the applied voltage V_t is chosen such that the limit $v_z \rightarrow 0$ occurs at $r=r_p$ within the inner well, just after positron and antiproton mixing commences. Next, assume that, outside of the inner well, the antiprotons have an axial drift velocity that is not a function of r . Then, the axial drift velocity within the inner well would be given by

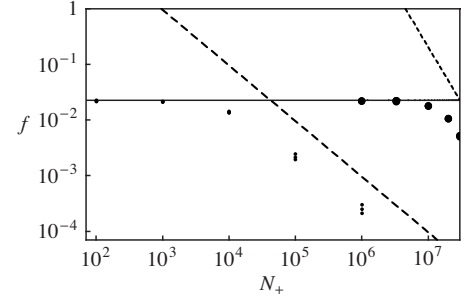


FIG. 2. Monte Carlo evaluation of the fraction of antiprotons with kinetic energies less than the maximum desirable energy E_{\max} versus the number of positrons N_+ using parameters reported by the ALPHA Collaboration [5] and with $r_p = 4$ mm. Three values of the fraction are computed for each value of N_+ to show the numerical convergence that occurs. (The three plotted points may not be distinguishable.) 100 000 phase-space-coordinate sets are sampled for computing each value of the fraction. The small dots are $f_{i\theta z}$ values. The large dots are $f_{i\theta}$ values, which are computed in the same way as $f_{i\theta z}$ values, except with $v_z = 0$. Equation (1) (straight solid line), Eq. (3) (short-dash line), and Eq. (5) (long-dash line) are shown for comparison.

$$v_z = \sqrt{\frac{e^2 \Delta n (r_p^2 - r^2)}{2\epsilon_0 m_-}}, \quad (4)$$

where the effect of positron space charge has been taken into account. Let $K_z = \frac{1}{2} m_- v_z^2$ denote the antiproton kinetic energy associated with an antiproton’s axial drift, where v_z is given by Eq. (4). The fraction of antiprotons for which K_z is less than E_{\max} within the positron plasma is given by

$$f_z = \frac{4\epsilon_0 E_{\max}}{e^2 \Delta n r_p^2}. \quad (5)$$

The two assumptions used to derive Eq. (4) represent optimal conditions, which maximize f_z . Also, notice that, with $\Delta n = n_+ = N_+ / (2\pi r_p^2 L)$, f_z is not a function of r_p .

Equations (1), (3), and (5) provide analytical expressions associated with thermal motion, azimuthal-drift motion, and axial-drift motion, respectively. The total fraction $f_{i\theta z}$ of antiprotons within the positron plasma that have a kinetic energy less than E_{\max} just after mixing commences is evaluated using a Monte Carlo phase-space sampling methodology. Phase space is sampled for a radially uniform antiproton distribution and a drifting Maxwellian velocity distribution, which is associated with a temperature $T_- = 4$ K and drift velocities given by Eqs. (2) and (4). The sampling expression used for the radial antiproton position in the guiding center approximation is $r = r_p \sqrt{R}$, where R is a random number that is equally likely to have any value between 0 and 1. Each velocity component is sampled using a conventional algorithm for sampling a Gaussian distribution with a standard deviation given by the thermal speed $\sqrt{kT_- / m_-}$ and a chosen mean. The mean is chosen to be v_θ as given by Eq. (2) for one velocity component, v_z as given by Eq. (4) for another velocity component, and 0 for the third velocity component. The results are plotted in Fig. 2 versus the number of trapped positrons N_+ for $r_p = 4$ mm. Equations (1), (3), and (5) are

shown for comparison. The comparison indicates that the dominant factors associated with $f_{i\theta z}$ are the antiproton thermal motion in the limit of small N_+ and the antiproton axial-drift motion for $N_+ \approx 3 \times 10^7$. It is found that $f_{i\theta z} \approx f_i = 0.022$ for $N_+ \lesssim 1000$ and $f_{i\theta z} < f_z = 3.2 \times 10^{-5}$ for $N_+ = 3 \times 10^7$.

A number of time-dependent processes will occur after mixing commences, and the system may evolve to have conditions suitable for producing significant numbers of antihydrogen atoms that may remain trapped. Experimental and theoretical studies have been reported regarding whether antiprotons reach a thermal equilibrium with positrons in a nested Penning trap before antihydrogen is formed, with varied conclusions [6–8]. It is illustrative to proceed with the assumption that antiprotons reach a thermal equilibrium with positrons faster than all other processes, and assume that the positron temperature does not increase. Then $v_z \rightarrow 0$, $f_z \rightarrow 1$, and the temperature of the antiprotons when located within the positron plasma would be equal to that of the positrons, $T_- = 4$ K. The fraction $f_{i\theta}$ of antiprotons within the positron

plasma that have a kinetic energy less than E_{\max} just after the antiprotons reach a thermal equilibrium with the positrons is evaluated using the Monte Carlo phase-space sampling methodology described above, except with $v_z = 0$. The results are plotted in Fig. 2. It is found that $f_{i\theta} \approx f_i = 0.022$ for $N_+ \lesssim 3 \times 10^6$ and $f_{i\theta} = 0.005$ for $N_+ = 3 \times 10^7$.

It is concluded that, for $N_+ = 3 \times 10^7$, $r_p = 4$ mm, and the rest of the parameters considered, the space charge of the positron plasma can have an important effect just after mixing commences and also after the antiprotons reach a thermal equilibrium with the positrons (assuming such a process takes place faster than all other processes and does not affect the positron temperature). The fraction of antiprotons that have an energy suitable for antihydrogen trapping can be substantially reduced by axial-drift motion and azimuthal-drift motion caused by the presence of positron space charge.

This material is based upon work supported by the Department of Energy under Grant No. DE-FG02-06ER54883.

-
- [1] M. Amoretti, C. Amsler, G. Bonomi, A. Bouchta, P. Bowe, C. Carraro, C. L. Cesar, M. Charlton, M. J. T. Collier, M. Doser, V. Filippini, K. S. Fine, A. Fontana, M. C. Fujiwara, R. Funakoshi, P. Genova, J. S. Hangst, R. S. Hayano, M. H. Holzschneider, L. V. Jorgensen, V. Lagomarsino, R. Landua, D. Lindelof, E. Lodi Rizzini, M. Macri, N. Madsen, G. Manuzio, M. Marchesotti, P. Montagna, H. Pruys, C. Regenfus, P. Riedler, J. Rochet, A. Rotondi, G. Rouleau, G. Testera, A. Variola, T. L. Watson, and D. P. van der Werf, *Nature (London)* **419**, 456 (2002).
- [2] G. Gabrielse, N. S. Bowden, P. Oxley, A. Speck, C. H. Storry, J. N. Tan, M. Wessels, D. Grzonka, W. Oelert, G. Schepers, T. Seifick, J. Walz, H. Pittner, T. W. Hansch, and E. A. Hessels, *Phys. Rev. Lett.* **89**, 213401 (2002).
- [3] M. Amoretti, C. Amsler, G. Bazzano, G. Bonomi, A. Bouchta, P. D. Bowe, C. Canali, C. Carraro, C. L. Cesar, M. Charlton, M. Doser, A. Fontana, M. C. Fujiwara, R. Funakoshi, P. Genova, J. S. Hangst, R. S. Hayano, I. Johnson, L. V. Jorgensen, A. Kellerbauer, V. Lagomarsino, R. Landua, E. Lodi Rizzini, M. Macri, N. Madsen, G. Manuzio, M. Marchesotti, D. Mitchard, F. Ottone, H. Pruys, C. Regenfus, P. Riedler, A. Rotondi, G. Testera, A. Variola, L. Venturelli, Y. Yamazaki, D. P. van der Werf, and N. Zurlo, *Phys. Lett. B* **583**, 59 (2004).
- [4] J. N. Tan, N. S. Bowden, G. Gabrielse, P. Oxley, A. Speck, C. H. Storry, M. Wessels, D. Grzonka, W. Oelert, G. Schepers, T. Seifick, J. Walz, H. Pittner, T. W. Hansch, and E. A. Hessels, *Nucl. Instrum. Methods Phys. Res. B* **214**, 22 (2004).
- [5] G. Andresen, W. Bertsche, A. Boston, P. D. Bowe, C. L. Cesar, S. Chapman, M. Charlton, M. Chartier, A. Deutsch, J. Fajans, M. C. Fujiwara, R. Funakoshi, D. R. Gill, K. Gomboroff, J. S. Hangst, R. S. Hayano, R. Hydromako, M. J. Jenkins, L. V. Jorgensen, L. Kurchaninov, N. Madsen, P. Nolan, K. Olchanski, A. Olin, A. Povilus, F. Robicheaux, E. Sarid, D. M. Silveira, J. W. Storey, H. H. Telle, R. I. Thompson, D. P. van der Werf, J. S. Wurtele, and Y. Yamazaki, *Phys. Rev. Lett.* **98**, 023402 (2007).
- [6] T. Pohl, H. R. Sadeghpour, and G. Gabrielse, *Phys. Rev. Lett.* **97**, 143401 (2006).
- [7] N. Madsen, M. Amoretti, C. Amsler, G. Bonomi, P. D. Bowe, C. Carraro, C. L. Cesar, M. Charlton, M. Doser, A. Fontana, M. C. Fujiwara, R. Funakoshi, P. Genova, J. S. Hangst, R. S. Hayano, L. V. Jorgensen, A. Kellerbauer, V. Lagomarsino, R. Landua, E. Lodi-Rizzini, M. Macri, D. Mitchard, P. Montagna, H. Pruys, C. Regenfus, A. Rotondi, G. Testera, A. Variola, L. Venturelli, D. P. van der Werf, Y. Yamazaki, and N. Zurlo, *Phys. Rev. Lett.* **94**, 033403 (2005).
- [8] F. Robicheaux, *Phys. Rev. A* **70**, 022510 (2004).